

## Review Article

Ulrike Fuchs\* and Sven R. Kiontke

# Breathing life into aspheric dreams

DOI 10.1515/aot-2016-0018

Received March 24, 2016; accepted June 3, 2016; previously published online June 25, 2016

**Abstract:** Introducing aspheric lenses in optical design broadens the horizons of possibilities and opens up new way to correct aberrations or creating effects that are not possible otherwise. Manufacturing these aspheric surfaces has come a long way during the last 15 years. This article discusses the state of the art concerning optical design, manufacturing, surface form tolerances and roughness to show the possibilities in hand.

**Keywords:** alignment; aspheres; large deviation; slopes; surface roughness.

## 1 Introduction

It has been more than 115 years since Ernst Abbe first thought about how aspheric optical surfaces could help in correcting aberrations. The utilization of conic surfaces dates back even further. Nevertheless, it has only been for the last 20 years that aspheric surfaces were considered a reasonable option in optical design, and it took another 10 to 15 years to improve the manufacturing processes in order to take them seriously for serial production. It has been a long way for aspheres to conquer the optical designer's toolbox for improving imaging systems by reducing aberrations or creating effects that are not possible otherwise. Due to the initial struggle of manufacturing such surfaces, there are still some misunderstandings about the possibilities and what to expect for tolerances. The aim of this article is to sort through this and show the state of the art of manufacturing aspheric surfaces. Thus, certitude of performance can already be gained within the optical design process.

\*Corresponding author: Dr. Ulrike Fuchs, Asphericon GmbH, Stockholmer Str. 9, 07747 Jena, Germany, e-mail: u.fuchs@asphericon.com

Sven R. Kiontke: Asphericon GmbH, Stockholmer Str. 9, 07747 Jena, Germany

[www.degruyter.com/aot](http://www.degruyter.com/aot)

© 2016 THOSS Media and De Gruyter

## 2 Optical design with aspheric surfaces

Of course, it is important for optical designers to be reasonable when designing new systems and keeping the overall cost of the final design in mind. Nevertheless, optical design tasks can be very challenging, and therefore it is important to keep an open mind for new approaches. Thus, employing aspheric surfaces in order to correct aberrations and reduce weight and length of an optical system are such opportunities. Aspheres are not the solution to all optical design problems, of course. For this reason, it is even more important to get a feeling for how aspheric surfaces act within an optical system. The surface description is given by

$$z(h) = \frac{h^2}{R \left( 1 + \sqrt{1 - (1+k) \frac{h^2}{R^2}} \right)} + \sum_{i=2}^n A_{2i} h^{2i}. \quad (1)$$

Focusing light with a singlet lens is the most trivial task but also a highly intuitive example to understand the way an aspheric surface acts. Figure 1 compares the two cases of focusing with a sphere and an asphere both having the same numerical aperture (NA). Of course, the asphere is the optical design dream due to the perfect focusing result, which is achieved locally, varying the radius of curvature of the first surface and therefore making it aspheric. It also gives a hint at how one can think of aspheric surfaces – as a localized zonal correction of the surface slope. Thus, when having more complex systems one should always ask whether the position of an aspheric surface is optimal for such a correction. Simultaneously, this also means that an aspheric surface can be placed at a position where it makes things worse. An example of this case is given in [1], discussing an Erfle eyepiece and its distortion correction with aspheric surfaces.

Laying out the design of a new optical system is usually less than half of the job. Putting tolerances on all optical and mechanical elements in order to achieve the needed as-built-performance later for the real optical system is the

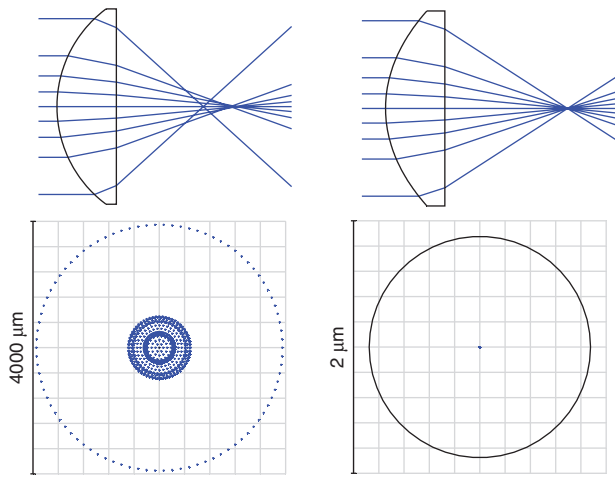


**Figure 1:** Top: A sphere (left) and an asphere (right) both having  $NA=0.54$  with  $D=25$  mm and effective focal length (EFL) 20 mm. For optimized focusing, the aspheric shape reduces the outer local radius of curvature. Thus, all rays meet in one focal point. The corresponding spot diagrams are depicted below. For the asphere the Airy-disc is shown as well since it is the natural limit for the focus spot size.

tough part, where a lot of experience is needed as well. A common way to model surface form deviation in optical design software packages is to either simulate them with low-order Zernike polynomials or to calculate the ray path deviation caused by first- and second-order aberrations. This is a very effective and powerful way to estimate form deviation of spherical surfaces. However, for aspheric surfaces it is a very limited prediction tool due

to the sub-aperture polishing employed in manufacturing and the characteristics of such real-world surfaces. Thinking of aspheric surfaces as local, zonal correction towards an optimized surface shape for a certain application also leads to a very intuitive way of putting tolerances on the surface form deviation. Since the local change in ray path is of interest, its deviation from the original design should be analyzed. The parameter to do so is the so-called slope deviation newly defined in ISO 10110-5 [2]. All mathematic background needed to calculate slope deviation is explained there.

Slope deviation can be measured either for a line scan (one-dimensional) or for a full surface measurement (two-dimensional). Both cases ask for a so-called window size and a sampling width. Defining both values creates a band-path filter, where the window size gives the upper limit for the spatial wavelength considered in a measurement and the sampling width defines the lower end. Figure 2 (right) gives an impression of how a two-dimensional slope map looks like. The corresponding surface form deviation is depicted in Figure 2 (left). It is possible to define multiple slope ranges for one surface, and even zonal definitions are allowed. The latter can also help saving costs by reducing manufacturing complexity.

Calculating slope deviation in optical design software packages needs some work-around, and one should also choose the performance criteria wisely. While high-order spatial frequencies have little effect on modulation transfer function (MTF) criteria, they can blur a spot

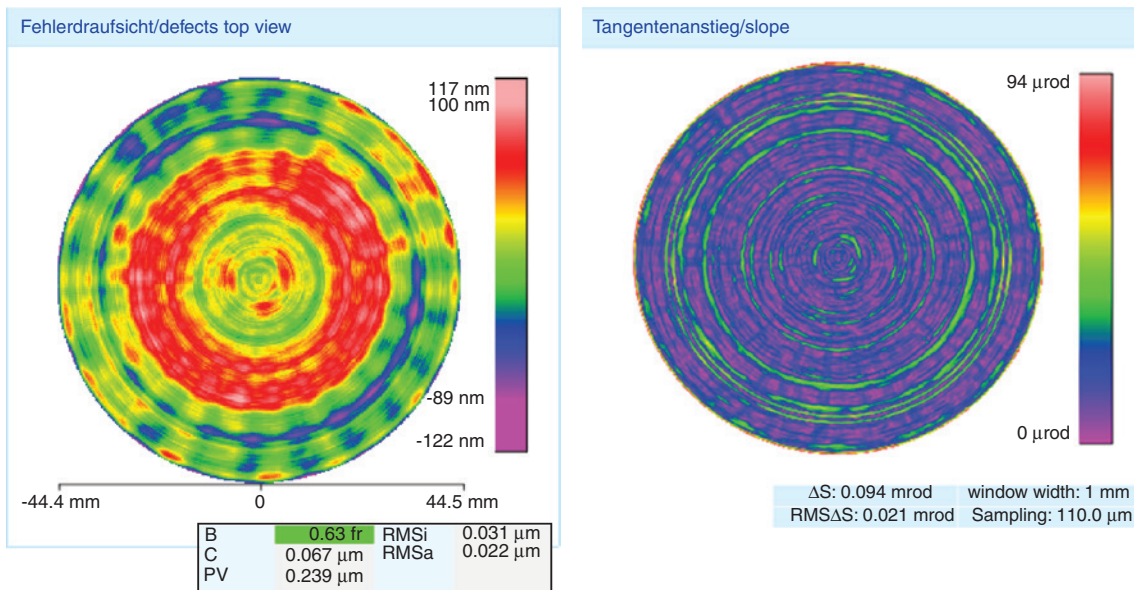


**Figure 2:** Example of a two-dimensional measurement for an aspheric surface showing the surface form deviation (left) and the corresponding slope deviation map (right). Additionally, all relevant data according to ISO 10110-5 are given.

significantly [3, 4]. To generate an educated guess on slope deviations that are of interest for a certain optical system,  $Q_{\text{bfs}}$  polynomials [5] can be employed. The surface description is given by

$$z(h) = \frac{h^2}{R \left( 1 + \sqrt{1 - \frac{h^2}{R^2}} \right)} + \frac{h^2 \left( 1 - \frac{h^2}{h_{\text{norm}}^2} \right)}{h_{\text{norm}}^2 \sqrt{1 - \frac{h^2}{R^2}}} \sum_{m=0}^M a_m Q_m^{\text{bfs}} \left( \frac{h^2}{h_{\text{norm}}^2} \right). \quad (2)$$

Figure 3 shows how the basic surface form and additional slope variations can be modeled this way [6, 7]. The aim was to create slope deviation of  $\text{RMS}\Delta S(80 \mu\text{rad}/1/0.1)$  and predict the decrease in focus quality. Observably the focus is blurred symmetrically, which is caused by the symmetry of the  $Q_{\text{bfs}}$ . Nevertheless, it is a fast and reliable way to look at slope deviation and the effects on the performance of an optical system. The slope deviation generated this way can also be used to derive more common values for surface form deviation, being  $3/0.45 (1.1) \text{RMSi } 78 \text{ nm}$  for this example. Note that this only works one way since slope deviation is a way to define how irregularity (IRR) is supposed to look like and is the stricter criterion.

### 3 Surface form and surface form deviation

At the very beginning of commercial production for aspheric surfaces based on computerized numerical control (CNC) grinding and polishing processes, measurement machines for this surface type were basically not available. One way was to use a computer generated holograms (CGH) with an interferometer or to rely on one-dimensional tactile scans. The former is extremely expensive and not very flexible; the latter limits the accuracy to about PV  $0.5 \mu\text{m}$ . Nowadays, these limitations have been overcome, and there are quite a few measurement techniques on the market, which can measure full surface form deviation of aspheric surfaces with basically no limitation to the surface shape. Without any claim of being complete, there are available several interferometers like ZYGO’s ‘Verifire™ Asphere’ (Zygo Corporation, Middlefield, CT, USA), QED’s ‘ASI(Q)’ (QED Technologies North America, Rochester, NY, USA) and Mahr’s ‘MarSurf TWI 60’ (Mahr GmbH, Göttingen, Germany), and pointwise scanning approaches like ‘LuphoScan’ (Ametek GmbH, Weiterstadt, Germany) Asphere metrology platform and Mahr’s ‘MarForm MFU

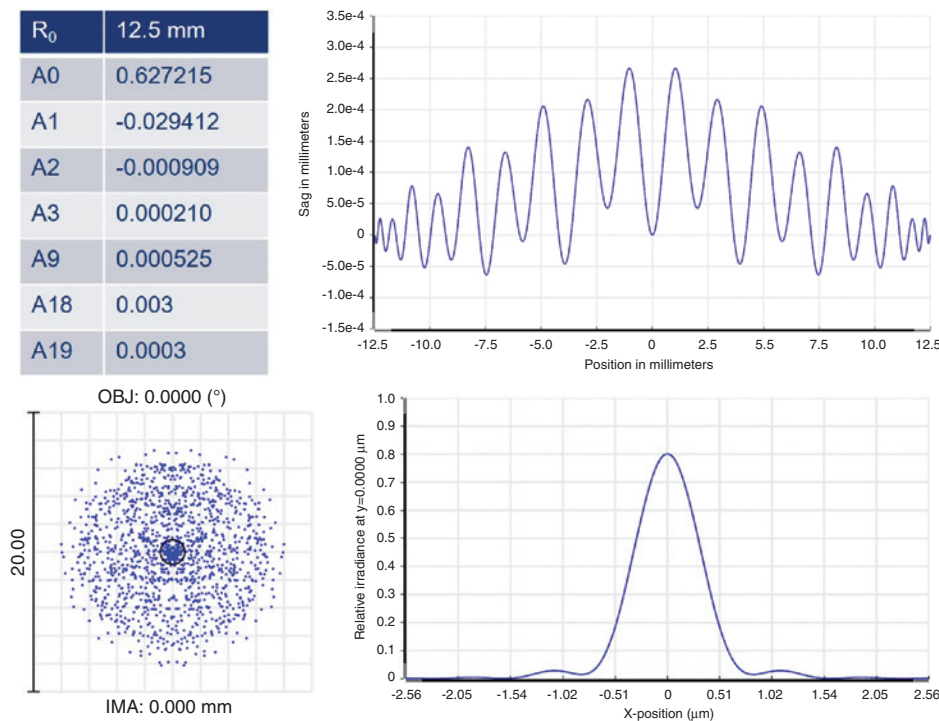


**Figure 3:** The first four coefficients in the upper left table describe the surface shape of the asphere depicted in Figure 1 (right) by using  $Q_{\text{bfs}}$ . The lower three coefficients create a slope deviation with  $\text{RMS}\Delta S(80 \mu\text{rad}/1/0.1)$ , and the resulting form deviation is depicted (top right). The corresponding surface form deviation would be  $3/0.45 (1.1) \text{RMSi } 78 \text{ nm}$ . The bottom figures depict the spot diagram with the Airy-disc (left) and the PSF in the focal plane (right).

200 Aspheric 3D'. Depending on the surface diameter, surface form deviation down to PV 50 nm can be measured. Also, measurement time is reasonably low with these approaches. The most important message from this development is that from this side of manufacturing there are basically no limitations regarding the surface form. The only thing that is still true is that for concave surfaces the smallest local curvature is limited by the radius of the tool used for grinding and polishing. Depending on the sub-aperture polishing technique employed, this is usually some value around 10 mm.

Another often cited recommendation refers to the so-called best fit sphere criteria for an aspheric surface. It states that if the departure from the best fit sphere increases significantly, the cost of manufacturing will rise dramatically. Well, this is only true when an aspheric surface is polished out of a sphere. Thus, the polishing time of that surface is proportional to the departure from the best fit sphere. Nowadays, it is common practice for high volume production to do aspheric grinding and therefore polish directly the surface shape required. This way it is possible to manufacture high surface form accuracy for reasonable prices. A very good example for this development and also for the possibilities it offers is the asphericon SPA Beam Expander Kit [8]. Due to the modular approach, all monolithic elements have to perform way above the common diffraction-limited criterion of Strehl  $> 0.8$ . The aim is to combine any five of those elements and still reach Strehl  $> 0.9$ . As shown in Figure 4 the measured wavefront meets this criterion perfectly. Thus, even though every other surface is aspheric it has a superior overall performance and shows what is already possible for serial production. Above this, single systems for space applications or similar challenging tasks can

reach even tighter specifications, especially when asking for very low surface roughness as discussed in the next section.

## 4 Surface roughness

Many applications require a high quality of roughness in order to reduce scattering, some of them in order to prevent from damage, like high-power laser applications. Others like spectrometers seek to increase the signal-to-noise ratio. Most of them have already been built with spherical surfaces. With higher demands on efficiency and more sophisticated versions, aspheric surfaces need to be employed. Therefore, the high requirement in roughness known from spherical surfaces is also needed on aspheric surfaces. For one thing, the constant change of curvature of an aspheric surface accounts for the superior performance; for another thing, it prevents using classical polishing techniques, which guaranteed this low roughness. New methods needed to be qualified.

Additionally, it has always been tricky to compare roughness values as different measurements often involved different filters, which then included or excluded certain spatial frequencies, which ends up in comparing apples and oranges. For measurements on aspheric surface this effect gets worse because of the sub-aperture polishing with small tools.

There are several methods to measure roughness. Tactile scanning methods occurred first. They are usually based on line measurements and especially useful for low frequencies of roughness error. For very high spatial frequencies, atomic force microscopy can be used. Because

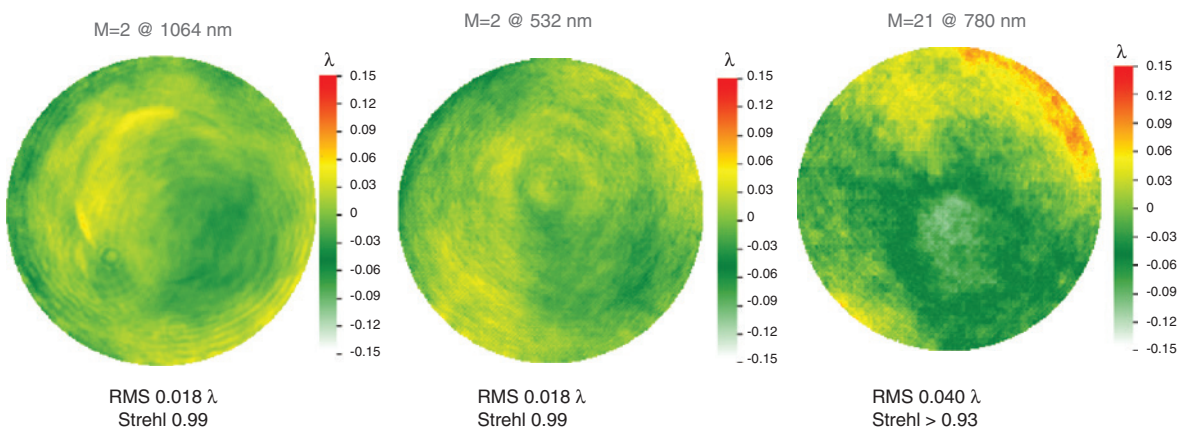


**Figure 4:** Wavefront measurements of two single SPA Beam Expanders at two different wavelengths having  $M=2$  magnification and a combination of five SPA Beam Expanders with  $M=21$ . All wavefront measurements are performed with a high-resolution Phasics sensor SID4-307c having  $300 \times 400$  pixel.

of a limited measurable window size ( $10\ \mu\text{m} \times 10\ \mu\text{m}$ ), it is limited to these higher frequencies. In between and even overlapping, a range of spatial frequency white light interferometry (WLI) is available. WLI is mainly used for the measurements and analysis shown below due to this characteristic.

For analysis usually RMS values are used, which can be calculated for a line measurement according to Eq. (3). The use of  $R_q$  is defined in the standards ISO4287 and ISO4288 (DIN4762, DIN4768). These versions are feasible for roughness measurements based on lines (one-dimensional) of measurement data.

$$R_q = \sqrt{\frac{1}{M N} \sum_{m=1}^M \sum_{n=1}^N (z(x_m, y_n) - \bar{z})^2} \quad (3)$$

$S_q$  and  $S_a$  are used for surface roughness analysis on two-dimensional basis. Area-based roughness analysis is defined in the standard ISO 25178. For  $A$  being the area of measurement, data  $S_q$  is defined as follows:

$$S_q = \sqrt{\frac{1}{A} \iint_A (z(x, y) - \bar{z})^2} \quad (4)$$

In addition to these two methods, it is possible to use filtering in order to address different spatial frequencies. Depending on the application, care has to be taken which frequencies are needed and which can be neglected. Figure 5 shows two measurements on exactly the same position and the same filter (0.001 mm) but with two different measurement areas: left ( $0.2\ \text{mm} \times 0.2\ \text{mm}$ ) and right ( $1\ \text{mm} \times 1\ \text{mm}$ ). The left measurement in Figure 5 shows a small  $S_q = 1.1\ \text{nm}$ . Extending the measurement area (Figure 1, right) increases the  $S_q = 5.2\ \text{nm}$  significantly. It is obvious that comparing roughness values only makes sense when the same filters were used. Consequently, roughness values without named filter values are very weak statements.

It is known that in aspheric production there is a much stronger presence of waviness. Often this is discussed as

part of surface form deviation. Aside from power, astigmatism and coma there are also many higher orders of deviations, caused by sub-aperture polishing. Now the question is whether this behavior might be also present in roughness and may be very strong in the lower roughness frequencies. The answer is yes and can be seen in Figure 5. Here a common pre-polishing of an aspheric surface is shown. In addition, it is obvious that especially the lower frequencies are worse than the rest. Thus, different manufacturing techniques (some available on the market) were analyzed with respect to their behavior on the different spatial frequencies with the aim to reduce the roughness dramatically over the full frequency range. Finally, two different approaches were successfully realized. The first attempt was to achieve high accuracy like  $\lambda/10$  with very low roughness. The second was focusing on series production of 100 units and more with the aim of reasonably priced production. Figure 6 shows the two corresponding results.

Both measurements show results in  $S_q$  of below 0.4 nm, which is at the limit of what WLI can measure and is remarkably low. This new manufacturing technique is capable of working at least until 0.5 mm spatial wavelength. This is a significant improvement compared to existing methods, which usually only reduce roughness of 0.1 mm spatial wavelength and below.

## 5 Mounting and alignment

To complete the task of setting up an optical system with one or more aspheric surfaces mounting and alignment is a challenging part as well. As mentioned before, aspheres can be interpreted as local correction for certain parts of the rays within a system. Thus, these surfaces can react quite critically to decenter and tilt tolerances. For a singlet focusing lens this can be relaxed by changing the optical

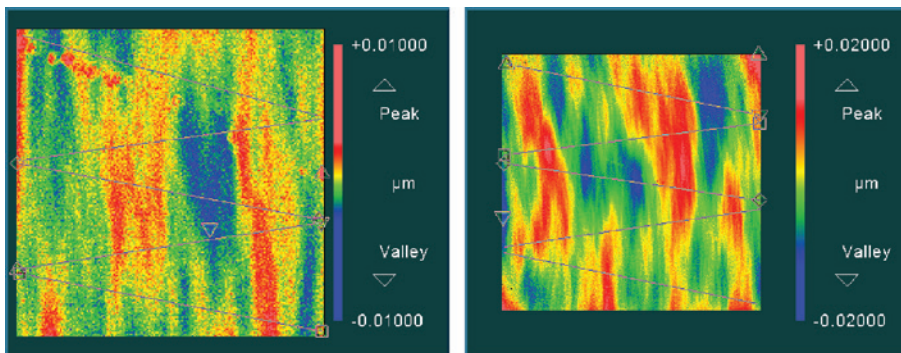


**Figure 5:** Same surface position with two different measurements: (left) filter 0.001/0.2 and  $S_q = 1.1\ \text{nm}$ ; (right) filter 0.001/1.0 and  $S_q = 5.1\ \text{nm}$ .

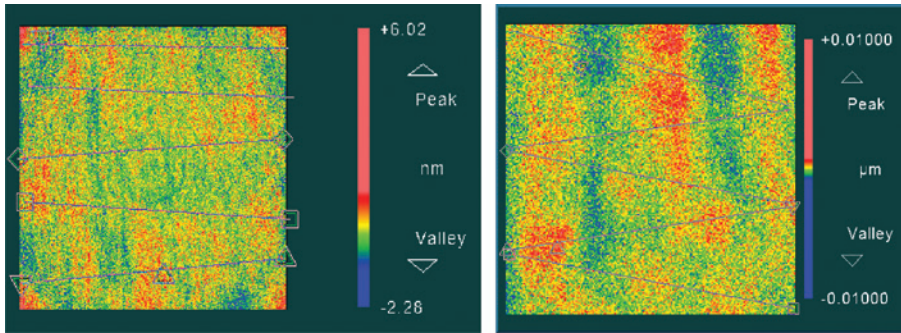


**Figure 6:** Two examples with very low roughness over a wide frequency range made by two similar approaches of manufacturing. Left: High-end form corrected lens ( $\lambda/10$ ): filter 0.001/1.0  $S_q=0.4$  nm; right: series production lens (>100 units per design/reasonable cost): filter 0.001/1.0  $S_q=0.3$  nm.

design from a plano-convex to a bi-convex element, using the sphere on the backside for a small field correction and therefore making it less sensitive to misalignment as shown in Figure 7. For more complex systems either this has to be balanced with more surfaces or the mounting technique has to be adapted. In contrast to spheres, which usually can be mounted easily with decenter tolerances in the region of  $50 \mu\text{m}$ , aspheres have to be placed much more precisely. Thus, common mounts with retaining rings cannot be employed for this purpose. One way of overcoming this limitation is to precisely glue the asphere into a high-precision mount that has datums by using e.g. an auto-collimation telescope for centering the lens to the mechanical axis, which is achieved by spinning the mount around its mechanical axis and shifting the lens within this mount until the detected decentration is minimized. This way decentration of  $<5 \mu\text{m}$  can be achieved.

Two other approaches would be alignment turning, where the mount is matched to the lens position by changing its outer shape [9], and centering aspheres in lens seat using retaining rings with specially designed threads [10].

## 6 Conclusion

In modern aspheric manufacturing, achievable surface form deviation and roughness are comparable to those known from classical spherical polishing processes. This opens up a completely new world for optical designers, which are no longer limited in shape and performance of aspheres. Of course, there are some specialties in tolerancing and mounting such optical systems, but solutions have been presented to overcome this as well. Above this, due to the significant improvements in manufacturing

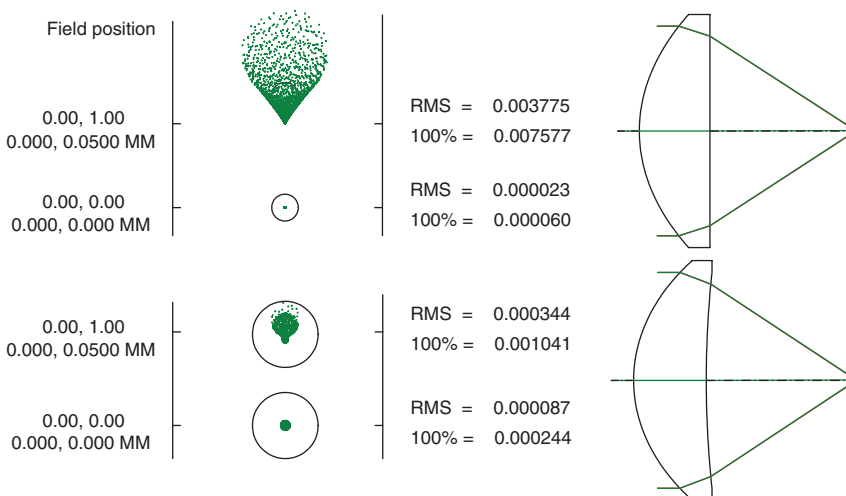


**Figure 7:** Comparing focal spots of two different layouts for an asphere having  $\text{NA}=0.54$  and  $\text{EFL}=20$  mm at two different field points, which correspond to on-axis focusing and tilting the lens by  $0.14^\circ$ . Employing the second surface curvature for field correction can reduce the alignment sensitivity significantly.

techniques and metrology, aspheric surface can be manufactured for reasonable prices and therefore become a serious option for real-world optics and leave their academic way of life. Based on this development, the next challenge is the so-called freeform surfaces, which offer even more degrees of freedom in optical design and therefore completely new applications.

## References

- [1] Asphericon GmbH, in Utilizing aspheres enhancement of optical performance using aspherical surfaces (Poster, Jena, 2015).
- [2] ISO 10110-5:2015 Surface form tolerances.
- [3] J. R. Rogers, Slope error tolerances for optical surfaces, Invited paper SPIE Technical Digest TD04-04 (2007).
- [4] J. R. Rogers, Slope sensitivities for optical surfaces. Proc. SPIE 9582, Optical System Alignment, Tolerancing, and Verification IX, 958206 (2015). Doi:10.1117/12.2186707.
- [5] G. W. Forbes, Opt. Express, 19, 9923–9942 (2011).
- [6] U. Fuchs, Tolerancing aspheric surfaces in optical design. Proc. SPIE 9582, Optical System Alignment, Tolerancing, and Verification IX, 958205 (2015). Doi:10.1117/12.2186405.
- [7] U. Fuchs, Better estimate of tolerances for aspheric surfaces in optical design, 10<sup>th</sup> International Conference on Optics-photonics, Weingarten (2016).
- [8] U. Fuchs, S. Wickenhagen, Modular optical design for flexible beam expansion. Proc. SPIE 9580, Zoom Lenses V, 958007 (2015). Doi:10.1117/12.2185914.
- [9] M. Beier, A. Gebhardt, R. Eberhardt and A. Tünnermann, Adv. Opt. Technol. 1, 441–446 (2012).
- [10] F. Lamontagne, N. Desnoyers, M. Doucet, P. Côté, J. Gauvin, et al., Disruptive advancement in precision lens mounting. Proc. SPIE 9582, Optical System Alignment, Tolerancing, and Verification IX, 95820D, (2015). Doi:10.1117/12.2196441.